Analyst

Accepted Manuscript

Isothermal Strand Displacement Amplification (iSDA): A Rapid and Sensitive Method of Nucleic Acid Amplification for Point-of-Care Diagnosis

Bhushan J. Toley*, Isabela Covelli, Yevgeniy Belousov[†], Sujatha Ramachandran, Enos Kline, Noah Scarr[†], Nic Vermeulen[†], Walt Mahoney[†], Barry R. Lutz, Paul Yager

Department of Bioengineering
University of Washington
Seattle, WA 98195-5061

† ELITechGroup Inc. Molecular Diagnostics
Bothell, WA 98021

Running Title: Isothermal strand displacement amplification (iSDA)

Keywords: Lateral flow assay, nicking enzyme, primer asymmetry, primer dimers, kinetic modeling, low resource settings

*Correspondence to:
Bhushan J. Toley
Department of Bioengineering
University of Washington
Box 355061, Foege N107
3720 15th Ave NE
Seattle, WA 98195-5061
Phone: 206-543-8063
Email: btoley@uw.edu

1

Abstract

We present a method of rapid isothermal amplification of DNA without initial heat denaturation of template, and methods and probes for a) real-time fluorescence detection and b) lateral flow detection of amplicons. Isothermal strand displacement amplification (iSDA) can achieve $>10^9$-fold amplification of the target sequence in <20 minutes at 49°C, which makes it one of the fastest existing isothermal DNA amplification methods. iSDA initiates at sites where DNA base pairs spontaneously open or transiently convert into Hoogsteen pairs, i.e. "breathe", and proceeds to exponential amplification by repeated nicking, extension, and displacement of single strands. We demonstrate successful iSDA amplification and lateral flow detection of 10 copies of a *Staphylococcus aureus* gene, NO.-inducible L-lactate dehydrogenase (*ldh1*) (Richardson, Libby & Fang, *Science*, 319: 1672-6, 2008), in a clean sample and 50 copies in the presence of high concentrations of genomic DNA and mucins in <30 minutes. We also present a simple kinetic model of iSDA that incorporates competition between target and primer-dimer amplification. This is the first model that quantitates the effects of primer-dimer products in isothermal amplification reactions. Finally, we demonstrate the multiplexing capability of iSDA by the simultaneous amplification of the target gene and an engineered internal control sequence. The speed, sensitivity, and specificity of iSDA make it a powerful method for point-of-care molecular diagnosis.

Introduction

Nucleic acid amplification tests (NAATs) are methods to rapidly diagnose pathogens directly by their DNA or RNA[1,2]. They offer several benefits over traditional culture-based approaches, particularly reduced test time (<2 hours compared to overnight cultures). Clinical sensitivities over 80% and specificities over 90% for detection of pathogens have consistently been reported using NAATs[3–6]. However, the most widely used method of conducting a NAAT, the polymerase chain reaction (PCR)[7], is not well suited to instrument-free point-of-care (POC) testing. POC testing is defined as testing near the patient, in a hospital, doctor's office, or at home, and is essential when a quick answer is desired or when appropriate facilities and supply chains are not available, such as in remote and low-resource settings[8]. Although PCR can be very sensitive, conducting PCR requires thermal cycling, a reliable source of electricity to power that, and trained technicians to conduct the test; this has limited the use of PCR in POC testing. To bridge this gap, several of the current authors participated in development of the Dx-Box – a small portable instrumented device that could perform both immunoassays and six PCR-based NAATs simultaneously[9]. The Dx-Box, which has yet to be commercialized, ran on a laptop battery for multiple runs. A successful commercial instrument, the Cepheid GeneXpert, bridges this gap to an extent by conducting a fully automated sample-to-result PCR-based NAAT without the need for trained technicians. However, the GeneXpert requires mains power, and the cost of the instrument and disposables can be prohibitive[10].

Isothermal NAATs (iNAATs) have emerged as viable alternatives to PCR. Because iNAATs, by definition, operate at a fixed temperature, they can be conducted in less complex and lower cost instruments more suited for POC NAATs. For example, iNAATs can be conducted in remote

3

locations using exothermic chemical reactions[11] or simply in hot water baths[12]. Several iNAAT methods, each with a unique way of initiating new rounds of DNA synthesis, have been developed and have been recently reviewed[13–17]. The best reported sensitivities of some widely used iNAAT methods (loop mediated isothermal amplification (LAMP)[18,19], recombinase polymerase amplification (RPA)[20], and strand displacement amplification (SDA)[21]) are ~10 copies of genomic DNA in absence of inhibitors. Several instruments have been designed exclusively for conducting diagnostic assays using an iNAAT method[22] including some commercial products[15]: Genie®II (OptiGene, UK) for LAMP, Twista® (TwistDx, UK) for RPA, and BD Probetec[TM] ET System (Becton-Dickinson, Franklin Lakes, NJ) for SDA.

For effective use in POC clinical diagnosis, an ideal iNAAT method must be fast, sensitive, specific, multiplexable, truly isothermal (initiation without heat denaturation); detection of amplicons should also be possible without sophisticated optical systems. Because current iNAATs typically operate at lower temperatures than PCR, they are prone to generate more non-specific amplification products, including primer dimers[23], that reduce their sensitivity[24–26]. Similarly, inhibitors from clinical samples reduce both speed and sensitivity of amplification reactions, e.g., the presence of 12.5 µg bovine mucin in a PCR reaction delayed the onset of the reaction by 2.4 cycles and 25 µg completely inhibited the reaction[27]. An ideal iNAAT method should be tolerant of typical inhibitors found in clinical samples and should be able to achieve good sensitivity in spite of non-specific side reactions. Generation of side amplification products also reduces the specificity of the assay if DNA-intercalating dyes are used for detection, in which case a detection signal is obtained even in absence of target[20]. Sequence-specific hybridization probes can eliminate this artifact. Another desirable feature of an ideal iNAAT

method is the ability to simultaneously amplify the target sequence and an internal control (IC) sequence in order to validate negative tests[28]. This is particularly important for POC tests, which may be conducted in low-cost minimally instrumented systems in the field. Many iNAAT methods, including LAMP and SDA, require initial heat denaturation of DNA at ~95°C followed by amplification at a lower temperature between 37 and 65°C, and are therefore not truly isothermal. For facilitating performance in the simplest instruments, an ideal iNAAT method should not require initial denaturation of template DNA. Finally, a minimally-instrumented method for amplicon detection would be ideal for POC use. Visually-detected lateral flow strips provide a non-instrumented detection system that meets this criterion and allows sequence-specific target detection.

In this paper, we describe a new method of DNA amplification called isothermal strand displacement amplification (iSDA) that meets the criteria of an ideal iNAAT method described above. The work described was carried out as part of a collaborative DARPA-supported project[†] aimed at developing a low-cost disposable instrument-free POC "platform" for detection of pathogens using iSDA (the MAD NAAT device). iSDA is a truly isothermal amplification method and does not require DNA denaturation for initiation. It is proposed that iSDA initiates by invasion of double-stranded DNA by a primer at DNA breathing sites[29,30]. We present the design and performance characteristics of an iSDA assay for the detection of *ldh1* gene for the detection of *S. aureus*[31]. iSDA can achieve ~10 copy sensitivity in <20 min. We also present sensitive and specific methods to detect amplicons in real-time as well as by a lateral flow assay. To better understand the competition between the specific amplification and primer-dimer

5

amplification reactions, we present a simple mathematical model of iSDA that predicts the shape of iSDA amplification curves with reasonable accuracy over a wide range of starting copy numbers. Finally, we demonstrate that iSDA can be successfully biplexed with an IC sequence. iSDA, coupled with appropriate sample conditioning, thermal control, and lateral flow detection, is fast, sensitive, and specific, and is therefore a promising method for conducting POC NAAT in a variety of platforms, and is ideal for use in low resource settings.

Materials and Methods

Enzymes, Primers and Probes

The nicking enzyme, Nt.BbvCI, and *Bst* 2.0 WarmStart DNA polymerase were purchased from New England Biolabs (NEB; Ipswich, MA). All primers and probes for real-time and lateral flow detection were designed and manufactured by ELITechGroup Inc. Molecular Diagnostics (Bothell, WA). Primer and probe sequences for *ldh1* and IC iSDA amplification are provided in Electronic Supporting Information (ESI) S1. Real-time fluorescence probes for *ldh1* and IC used FAM and AquaFluor® 525 (AP525; A Trademark of ElitechGroup S.A.S.) fluorophores, respectively.

iSDA Amplification

Purified genomic DNA from methicillin-resistant *Staphylococcus aureus* (MRSA) was obtained from ATCC (BAA-1556). All iSDA reactions were conducted in a Rotor-Gene Q (Qiagen, Valencia, CA) held at 49°C for 30 minutes. Each 10 μl *ldh1* iSDA reaction contained 50 mM potassium phosphate, 3.8 mM magnesium sulfate, 200 μM of each dNTP, 250 nM extension primer E1, 500 nM extension primer E2, 50 nM each of bumper primers B1 and B2, 8 units of

polymerase, 1.6 units of nicking enzyme, and 0.84 µl diluent A (NEB). Two types of reactions were conducted: i) for generating real-time amplification curves, and ii) for lateral flow detection. For real-time amplification curves, Pleiades probe[32] (ELITechGroup, Bothell, WA) at 200 nM was used, and for lateral flow detection, 200 nM each of biotin probe (ELITechGroup Inc., Bothell, WA) (5'-Biotin Phosphoramidite 10-5950-95 Glen Research, Sterling Virginia USA) and capture probe (ELITechGroup Inc., Bothell, WA) were used. For *ldh1* + IC biplex reactions, additional primers and probes for the IC were added at the following concentrations: extension primers $E1_{IC}$ and $E2_{IC}$ at 500 and 250 nM respectively, bumper primers $B1_{IC}$ and $B2_{IC}$ at 50 nM each, and Pleiades probe at 200 nM. The final volume of each reaction was adjusted to 10 µl by adding water. Fluorescence signals were acquired every minute in the green channel of the Rotorgene for *ldh1* and yellow channel for the IC, at a gain setting of 10. The maximum fluorescence intensity reached by no-template control (NTC) reactions at 30 min was set as the threshold value for calculating lift-off time, C_t. Reactions were set up by adding 1 µl DNA template solution, 7 µl mixture of all reactants excluding enzymes, and 2 µl mixture of enzymes and diluent A, in that order. After addition of components, tubes were vortexed for 3-5 s for effective mixing using a pulsing vortex mixer (Fisher Scientific, Waltham, MA) and were spun in a mini centrifuge (Fisher Scientific) for 2-3 s to collect fluid from the walls of the tubes, before transferring to the Rotor-Gene.

Lateral Flow Detection

Pyranosyl-DNA (pDNA) is a modified form of DNA that does not bind to conventional DNA and forms duplexes that are more stable than their conventional DNA counterparts[33]. The capture probe for lateral flow was a pDNA probe linked to T20 (twenty repeats of thymidine). A

400 μM capture probe solution in water was striped along the length of a 30 cm x 2.5 cm cardboard-backed nitrocellulose FF80HP (GE Healthcare, Waukesha, WI) sheet at 0.3 μl/cm at ambient temperature and humidity using a BioDot (Irvine, CA) striper. A control line of 200 μM T20-biotin was striped at equal flow rate and placed parallel to and downstream of the test line. The sheet was placed over a UV light source using a UVC transilluminator TM-36 (Upland, CA) to induce crosslinking, which renders the capture probes immobile on the nitrocellulose[34,35]. After drying, a cellulose CFSP203000 (Millipore, Billerica, MA) wicking pad, 30 cm x 2 cm, was adhered to one edge of the nitrocellulose sheet. Detection strips, ~ 4 mm wide, were scissor-cut from this assembly. During detection, 5 μl out of the 10 μl reaction volume was mixed with 100 μl of lateral flow buffer containing 0.4 M NaCl, 1% Triton X-100, 0.5% BSA, 15 mM HEPES, 0.01% w/v streptavidin-coated 190 nm diameter polystyrene blue beads (Bangs Laboratories, CP01B, Fishers, IN), adjusted to pH 7.1. The high salt concentration is used to improve pDNA-pDNA binding at the test line. The 105 μl solutions were introduced into individual wells of a deep 96 well plate (VWR, Radnor, PA), and a detection strip was introduced into each well. Strips were removed from the well and scanned after 20 minutes using an Epson (Long Beach, CA) Perfection V700 flatbed scanner at 600 dpi RGB color, 16-bit depth per color channel. Normalized integrated test line intensities, I_{test}, were obtained from scanned strips using a procedure described in ESI S2. Two-tailed Student's *t*-tests were used for statistical comparisons.

Polyacrylamide Gel Electrophoresis (PAGE)

See ESI S3.

Kinetic Reaction Network Modeling

The chemical network to be modeled was first represented as a set of chemical reactions. For enzymatic reactions, substrate and enzyme were assumed to reversibly form an enzyme-substrate complex, which irreversibly degraded into product and regenerated the enzyme[36,37]. The law of mass action was used to set reaction rates and the model was solved in MATLAB (MathWorks, Natick, MA) using the Systems Biology Toolbox[38]. All reaction rate constants (except the rate of primer dimer formation and the rate of annealing of sense and antisense amplicons) were obtained from literature by selecting rate constants of similar reactions. Details of model solution are provided in ESI S4.

Simulated Nasal Matrix

An FDA-approved simulant of nasal samples was used to challenge iSDA reactions. Simulated nasal matrix (SNM) contained 110 mM NaCl, 1% w/v Type III mucin from porcine stomach (Sigma-Aldrich, M1778, St. Louis, MO), and 10 μg/ml human genomic DNA (Promega, G3041, Madison, WI) in water[39]. These components mimic the composition of a human nasal swab sample.

Results and Discussion

Molecular Mechanism of iSDA

iSDA is orchestrated by two enzymes: i) a nicking enzyme, Nt.BbvCI, that creates a single stranded nick in the double-stranded DNA sequence 5'—CC TCAGC—3' at the location marked by ' ', and ii) DNA polymerase, *Bst* 2.0 WarmStart, that has strong 5'$\rightarrow$3' strand displacement activity but that lacks 5'$\rightarrow$3' exonuclease activity. There are two pairs of primers: a

pair of flapped primers or extension primers, E1 and E2, and a pair of bumper primers, B1 and B2. The flap, a portion of the 5' end of extension primers, is not complementary to the target sequence and these non-complementary sequences contain the sequence recognizable by the nicking enzyme, i.e. a nicking site (*Legend*, Fig.1). Unlike SDA, iSDA does not require initial DNA heat denaturation. Instead, amplification presumably initiates at sites of DNA breathing[29].

There are two phases of amplification: pre-exponential (Fig. 1A) and exponential (Fig. 1B). Pre-exponential amplification starts with genomic DNA (lacking an Nt.BbvCI nicking site in the *ldh1* gene) and generates a double-stranded product with nicking sites on both strands. Only the polymerase is utilized in this phase; the nicking enzyme does not participate. A primer anneals to a DNA breathing site in genomic DNA (holding it open) and is extended by the polymerase to displace a single strand, S1 (Fig. 1A). Primers E1 and B1 then bind to S1. The extension of E1, followed by extension of B1, displaces another single strand, S2, the 5' end of which has the same sequence as primer E1 (Fig. 1A). Primers E2 and B2 now bind to S2 and in a similar manner, their extension displaces a single strand, S3, the 5' end of which has the same sequence as primer E2 (Fig. 1A). The 3' end of S3 is fully complementary to E1. E1 then anneals to S3 and its extension produces a double-stranded product, D, which has a nicking site on both strands (Fig. 1A). This concludes the pre-exponential phase and creates the double-stranded product with nicking sites at both ends needed for exponential amplification.

The exponential phase of the reaction involves synchronous action of the nicking enzyme and polymerase (Fig. 1B). The nicking enzyme can act on both nicking sites in D, producing nicked products $D_{N,A}$ and $D_{N,B}$ (Fig. 1B). The polymerase extends these nicked strands in the 5' → 3'

direction to regenerate D and displace single strands, $S1_A$ and $S1_B$. Hybridization probes are designed for the sense strand, $S1_A$. Sense and antisense strands are color coded black and grey, respectively, in Figure 1B. $S1_A$ and $S1_B$ then anneal to primers E1 and E2 and their extension generates double strands, $D1_A$ and $D1_B$, respectively (Fig. 1B). $D1_A$ and $D1_B$ have only one intact nicking site. Nicking and extension from these sites regenerates $D1_A$ and $D1_B$ and produces two new single strands, $S2_A$ and $S2_B$. Note that hybridization probes can detect $S2_B$, but not $S2_A$. Primers E1 and E2 then bind to $S2_B$ and $S2_A$ to regenerate the intermediate species, $S1_A$-E1 and $S1_B$-E2, respectively, thus completing the loop. Multiple cycles of these reactions lead to exponential amplification. Detectable products of two different lengths are generated: uncut products, $S1_A$ and $S1_A$-E1, and cut products, $S2_B$ and $S2_B$-E1. For the *ldh1* iSDA assay, the uncut and cut products, $S1_A$ and $S2_B$, are 121 and 101 bases long, respectively.

In order to detect amplicons using hybridization probes, it is necessary to generate single-strand products. Note that $S1_A$, $S2_A$, $S1_B$, and $S2_B$ have long complementary sequences. If the left and right reaction cascades in Fig. 1B, initiating from $D_{N,A}$ and $D_{N,B}$, respectively, generate equimolar products, these single strand will preferentially anneal to each other and not to the probes. To allow detection by hybridization probes, in this embodiment of iSDA, a lower (and hence) limiting concentration of primer E1 is used to generate more $S2_B$ than $S2_A$. Depending on the probe types used, detection can be conducted using two methods: a) real-time fluorescence detection, or b) lateral flow detection. Real-time detection is carried out here using ELITechGroup's Pleiades probes[32], which are DNA probes that have a fluorophore and a minor groove binder at the 5' end and a quencher at the 3' end (Fig. 2A). The fluorophore is quenched in the unbound state and fluoresces when hybridized to the target. For lateral flow detection, a

twin-probes approach is used to allow capture and labeling (note that the nicking mechanism does not allow capture or detection using end-labeled primers) (Fig. 2B). In this approach, probes are designed for two different regions of the amplicon. One probe (the detection probe) is biotinylated at the 3' end and enables conjugation with streptavidin-coated detection particles. The other probe (the capture probe) is a 5'-pDNA-DNA-3' chimera, the DNA part of which is complementary to the amplicon, and the non-complementary pDNA part is used for capture on a surface to an immobilized complementary pDNA probe (Fig. 2B). The requirement for two sequence-specific binding events increases specificity.

iSDA Amplification of MRSA DNA

iSDA amplification was conducted with different numbers of copies of purified MRSA genomic DNA as the detection target. Real-time amplification curves for 0 (no template control; NTC), 50, 250, and 1000 copies are shown in Fig. 3A. Curves show the mean values of 3 reactions and error bars represent standard deviation. All curves, except the NTC, lifted off at ~8 minutes and plateaued before 20 minutes. The plateau level, which represents the number of detectable asymmetric amplicons, increased with increasing starting copies. At 20 minutes, the number of amplicons formed for 1000 input copies was significantly greater than for 250 and 50 copies (*; $P<0.05$; Fig. 3A). Similarly, the number of detectable amplicons formed at 20 minutes for 250 copies was significantly greater than for 50 copies (*, $P<0.05$; Fig. 3A). For 10 copies, amplification curves lifted above NTC levels, but the curves were variable with a large standard deviation (not shown).

A set of experiments was also conducted with lateral flow probes and lateral flow detection. Fig. 3B shows lateral flow detection of amplicons starting from 0 (NTC), 10, 50, 250, and 1000 copies of *ldh1* in replicates of three. The direction of fluid flow on the detection strips is indicated in Fig. 3B; fluid ultimately flowed into a cellulose wicking pad. The first line in the flow path was a 'test' line for capturing amplicons (pDNA probe) and the second line was a 'control' line for capturing blue beads (immobilized biotin). The control line was visible on all strips. For NTC runs, there was no visible test line, as expected, and test lines were visible (positive) for 10, 50, 250, and 1000 copies (Fig. 3B). All positive test lines were dark enough to be detected by naked eye, except one replicate at 10 copies. Average I_{test} increased with increasing starting copies (Fig. 3C) over the range of *ldh1* input copies tested. The average I_{test} for 1000 copies was significantly greater than 250 copies, which was significantly greater than 50 copies (*;P<0.05; Fig. 3C). For 50, 250, and 1000 copies, average I_{test} was significantly greater than NTC (*;$P<5 \times 10^{-4}$; Fig. 3C). For 10-copy inputs, the average I_{test} was not significantly greater than NTC because one strip had a weak signal.

The reduction in detectable product at low input copies is, we believe, a result of competition for primers and dNTPs by side reactions, including primer dimer amplification. This competition between amplification of target and amplification of off-target hybrids and primer dimers is well demonstrated by denaturing PAGE analysis of products of iSDA reactions (Fig. 3D). The target amplification bands are at 101 and 121 nucleotides (red arrows; Fig. 3D). There were no target bands for NTC reactions. In the presence of template, the intensity of target bands increased with increasing copies (Fig. 3D). Besides target bands, there were multiple bands of lower molecular weight. Because these bands are formed for NTC reactions also, they must be template-

independent and the result of primer and probe side reactions. For example, if primers E1 and E2 had some non-specific interactions near their 3' end, their extension would lead to a double-strand product with nicking sites on both strands, similar to product D (Fig. 1B). This primer dimer is amenable to rapid exponential amplification because of its small size. There were two distinct bands of ~47 and 67 nucleotides (yellow arrows; Fig. 3D) that most likely correspond to primer dimer amplification reactions ensuing from a 2 base pair overlap in primers E1 and E2. These bands were brightest for NTC and least bright for 1000 copies (Fig. 3D).

Although this iSDA reaction is already fast and sensitive, reducing primer-related side amplification reactions further improves the performance of iSDA. We have observed that amplification in the absence of the *ldh1* target for ~1 minute generates enough side products that when the target is added at ~1 min, side products have taken over and the target is not amplified. Similarly, if an iSDA reaction is contaminated with the products of a previously conducted NTC iSDA reaction, the reaction produces a false negative result because amplification of "NTC products" outcompetes target amplification (see ESI S2). It is important to understand these competing processes well in order to avoid these problems and further improve iSDA.

Simplified Mathematical Model of iSDA

A mathematical model of iSDA was created primarily to understand the effects of primer-mediated side amplification reactions on the main amplification pathway. The mathematical model represents iSDA with the simplest and most representative chemical reactions. For target amplification, initial steps that occur during the pre-exponential stage are not included because it is assumed that every copy of DNA template rapidly produces one copy of species D (see Fig.

1A). Exponential amplification is considered the main amplification pathway of iSDA. In this simplified model, the two products of different lengths generated by iSDA are considered equivalent and all primer-mediated side reactions are represented by a single primer-dimer amplification reaction initiating from binding of the two extension primers, E1 and E2, near their 3'end.

Fig. 4A shows the modeled simplified schematic of target amplification by iSDA. Species D' has nicking sites (dotted blue regions; Fig. 4A) in both strands and marks the beginning of the exponential phase of the reaction. D' is nicked to produce DAN' and DBN', from which, single strands SA (sense) and SB (antisense), respectively, are displaced. SA and SB anneal to primers E1 and E2, respectively, which extend to generate double-stranded products that would be shorter than D', but in this simplified model, assumed to be equivalent to D'. The complementary amplicons SA and SB can also anneal to generate SA-SB (dotted arrows; Fig. 4A), which does not participate in further amplification. A fluorescent probe, F, binds to the sense strand, SA, to generate SA-F, which in turn binds to primer E1 to generate SA-F-E1 and extends to regenerate D'. Probe-bound species, SA-F and SA-F-E1 are detected in real time amplification curves.

Fig. 4B shows the modeled schematic of a primer-dimer amplification reaction. Extension primers E1 and E2 anneal near their 3' ends and are extended to generate a double-stranded product, P, which has nicking sites in both strands. P, similar to D' (Fig. 4A), can undergo exponential amplification, generating nicked products PAN and PBN, single strands SPA and SPB, which anneal with primers to generate SPA-E2 and SPB-E1, and a dead end product, SPA-

SPB (Fig. 4B). None of the primer-dimer amplification products are detectable by fluorescent probes because they lack the target-specific interior probe-binding region.

Real-time amplification curves predicted by the model (Fig. 4C) matched experimentally observed curves (averages of three runs) very well (Fig. 4D). The relative fluorescence units of experimental curves were converted into concentrations (nM) using a fluorescence-concentration calibration performed separately (ESI S5). The model captures a few important characteristics of the experimental real-time curves: i) it accurately predicts the lift-off times of the curves between 7-10 min and predicts that curves for higher input copies lift-off earlier (Fig. 4C,D), and ii) it accurately predicts the trend of plateau levels of the curves, i.e., plateau levels increase with increasing input copy numbers, but are equal for 1000 and 10,000 input copies. Further validation of the model is presented in ESI S4.

The model was used to calculate the concentration-time profile of primer dimer amplification products. Fig. 4E shows the sum of concentrations of species P, PAN, PBN, SPA, SPB, SPA-E2, SPB-E1, and SPA-SPB over time. The NTC starting condition produces the maximum number of side products, and the number of side products decreases as the number of target copies increases, which is consistent with the gel results shown in Fig. 3D. Finally, the model was used to predict the shape of amplification curves in a hypothetical case where side reactions were absent (rate of primer-dimer formation was set to zero; Fig. 4F). In this scenario, equal numbers of target products are generated, independent of the number of starting copies (Fig. 4F). This is similar to PCR reactions that typically have a negligible rate of non-specific amplicon

generation. This suggests that the sensitivity of iSDA can be further improved by reducing the rate of primer self-association.

Effect of contaminants on iSDA

The *ldh1* assay was developed for diagnosis of *S. aureus* in human nasal swabs. The tolerance of the iSDA reaction to human genomic DNA (hgDNA) and SNM was therefore tested. As much as 10 ng hgDNA did not have a negative effect on amplification as seen by average amplification curves for 50 and 1000 copies (N=3) in the presence of 0 or 10 ng hg DNA (Fig. 5A). In a separate experiment, amplification followed by lateral flow detection of NTC, 50, 250, and 1000 copies was tested in the presence of 0, 5, or 10 ng hgDNA. Dark lateral flow signals were obtained in all conditions (Fig. 5B). The presence of 5 and 10 ng hgDNA did not significantly reduce I_{test} at any copy number (Fig. 5C).

Next, iSDA was conducted in the presence of 10% SNM (10 ng hgDNA and 10 μg mucin per 10 μl reaction). Average amplification curves (N=3) for 250 and 1000 copies in the presence of 0 or 10% SNM are shown in Fig. 5D. The presence of 10% SNM delayed the onset of curves as well as reduced the plateau level. The cycle time, C_t, at which amplification curves reached above the threshold intensity value significantly increased from an average of 7.3 to 13.3 minutes for 1000 copies, and from 8 to 16.7 minutes for 250 copies (*;P<0.05; Fig. 5E). For 50 copies, only 1 out of 3 amplification curves lifted above threshold (not shown). Nonetheless, in the presence of 10% SNM, lateral flow signals visible by eye were obtained for 2 out of 3 reactions containing 50 copies and for all replicates of 250 and 1000 copies (Fig. 5F). With 10% SNM, I_{test} reduced significantly for 50 and 250 copies (*; P<0.05), but not for 1000 copies (Fig. 5G).

Biplex iSDA Amplification

We next demonstrated simultaneous amplification of the *ldh1* gene and an engineered single-stranded IC sequence in the same reaction. Amplification of 0, 100, 500, and 5000 copies of *ldh1* was conducted in the presence of 2500 copies of IC. Controls included NTC, *ldh1* positive control (5000 *ldh1*; 0 IC), and IC positive control (2500 IC; 0 *ldh1*). Average real-time amplification curves (N=3) for *ldh1* (green channel) and IC (yellow channel) are shown in Fig. 6A and Fig. 6B, respectively. All copy numbers of *ldh1* were successfully amplified in the presence of 2500 IC copies (Fig. 6A). The lift-off times of the curves decreased and plateau levels of the curves increased with increasing *ldh1* copy number (Fig. 6A). Similarly, 2500 IC copies amplified successfully at all *ldh1* copy numbers (Fig. 6B). However, the lift-off times of the curves increased marginally and plateau levels decreased with increasing number of *ldh1* copies, demonstrating the competition for dNTPs between the two amplification pathways. NTC curves did not lift off in either detection channel (Fig. 6A,B). There was no fluorescence bleed between the two channels, i.e., the amplification curve for *ldh1* positive control did not lift off in the yellow channel and vice versa (brown curves; Fig. 6A,B). Amplification of IC produces two products of length 91 and 111 nucleotides (yellow lines; column 2; Fig. 6C). With increasing number of *ldh1* copies, brighter *ldh1* product bands were obtained (green lines; columns 3-4; Fig. 6C). At 5000 *ldh1* and 2500 IC copies, four amplification products – two each for *ldh1* and IC – were clearly seen on the gel (column 4; Fig. 6C). In absence of IC, only *ldh1* product bands were obtained (column 5; Fig. 6C). NTC did not produce any of the four products (column 1; Fig. 6C).

There is an inherent competition between amplification of target (*ldh1*) and the IC in biplex reactions. The sensitivity of the biplex assay to the target may be improved further by reducing the number of IC copies, thus shifting the competition in the favor of the target. If the target is present and amplifies successfully, then failure to amplify the IC is acceptable. However, the number of IC copies should not be so low that IC amplification fails in the absence of target. The choice of the number of IC copies is therefore a critical tradeoff.

The sensitivity of biplex amplification may further be affected by non-specific amplification pathways. Biplex amplification produced more side product bands (Fig. 6C) than *ldh1* alone (Fig. 3D). This is expected because of cross reactivity between the additional primers. Careful primer design that minimizes these secondary interactions between primers is critical for the design of all biplex reactions, including biplex PCR reactions. In the system described above, a wide dynamic range of 100-5000 target copies with successful IC amplification by iSDA was demonstrated.

Conclusions

iSDA is a powerful method of isothermally amplifying target DNA strands exponentially in 20-30 minutes, and is resistant to some common inhibitors found in clinical samples. Combined with high-specificity probes for lateral low detection and design of instrumentation that can take advantage of this, iSDA promises to reduce the cost of molecular diagnosis by eliminating the need for using expensive instruments. Reactions can be conducted in water baths or inexpensive portable heat packs followed by paper-based lateral flow detection. iSDA is an enabling technology for the current DARPA-funded project in which we participate that is aimed at

developing portable instrument-free sample-to-answer molecular test devices for POC pathogen detection. Through this work, we recognized that primer-dimer products reduce the amount of target amplicons generated by iSDA starting from low target copies and we quantified this effect. Despite these primer-dimer reactions, iSDA can achieve remarkable speed and sensitivity. Further improvement in primer design and reaction conditions could reduce this primer dimer interaction and further improve the sensitivity of iSDA; performance comparable to PCR could be achieved in the future. Future work from this group will report on the use of iSDA for amplification of other DNA and RNA targets from intact pathogens and on more detailed mathematical models of iSDA that will enable optimization for maximum detectable product generation.

Acknowledgment

References

1   A. Y. Vittor, J. M. Garland and R. H. Gilman, *Ann. Glob. Heal.*, 2014, **80**, 476–485.

2   P. Behzadi, R. Ranjbar and S. M. Alavian, *Jundishapur J. Microbiol.*, 2014, **8**, 1–7.

3   L. Kivihya-ndugga, M. Van Cleeff, E. Juma, J. Kimwomi, W. Githui, L. Oskam, D. Van Soolingen, L. Nganga, J. Odhiambo, P. Klatser, A. Schuitema and D. Kibuga, 2004, **42**, 3–7.

4   L. E. Scott, K. McCarthy, N. Gous, M. Nduna, A. van Rie, I. Sanne, W. F. Venter, A. Duse and W. Stevens, *PLoS Med.*, 2011, **8**, 1–11.

5   J. L. Davis, L. Huang, J. a Kovacs, H. Masur, P. Murray, D. V Havlir, W. O. Worodria, E. D. Charlebois, P. Srikantiah, A. Cattamanchi, C. Huber, Y. R. Shea, Y. Chow and S. H. Fischer, *Clin. Infect. Dis.*, 2009, **48**, 725–732.

6   X. Chen, Q. Yang, H. Kong and Y. Chen, *Int. J. Tuberc. Lung Dis.*, 2012, **16**, 235–239.

7   L. Garibyan and N. Avashia, *J. Invest. Dermatol.*, 2013, **133**, 392–395.

8   O. Clerc and G. Greub, *Clin. Microbiol. Infect.*, 2010, **16**, 1054–1061.

9   P. Yager, G. J. Domingo and J. Gerdes, *Annu. Rev. Biomed. Eng.*, 2008, **10**, 107–44.

10   C. A. Evans, *PLoS Med.*, 2011, **8**.

11   K. a. Curtis, D. L. Rudolph, I. Nejad, J. Singleton, A. Beddoe, B. Weigl, P. LaBarre and S. M. Owen, *PLoS One*, 2012, **7**, 1–6.

12   J. Sirichaisinthop, S. Buates, R. Watanabe, E. T. Han, W. Suktawonjaroenpon, S. Krasaesub, S. Takeo, T. Tsuboi and J. Sattabongkot, *Am. J. Trop. Med. Hyg.*, 2011, 85, 594–596.

13   A. Niemz, T. M. Ferguson and D. S. Boyle, *Trends Biotechnol.*, 2011, **29**, 240–250.

14   M. K. Motamedi, M. Saghafinia, A. Karami and P. Gill, *J. Glob. Infect. Dis.*, 2011, **3**, 293.

15   P. Craw and W. Balachandran, *Lab Chip*, 2012, **12**, 2469.

16   J. Li and J. Macdonald, *Biosens. Bioelectron.*, 2015, **64**, 196–211.

17   H. Deng and Z. Gao, *Anal. Chim. Acta*, 2015, **853**, 30–45.

18   T. Notomi, H. Okayama, H. Masubuchi, T. Yonekawa, K. Watanabe, N. Amino and T. Hase, 2000, **28**.

19   Z. K. Njiru, *PLoS Negl. Trop. Dis.*, 2012, **6**, 1–4.

20   O. Piepenburg, C. H. Williams, D. L. Stemple and N. a. Armes, *PLoS Biol.*, 2006, **4**, 1115–1121.

21   G. T. Walker, M. S. Fraiser, J. L. Schram, M. C. Little, J. G. Nadeau and D. P. Malinowski, *Nucleic Acids Res.*, 1992, **20**, 1691–1696.

22   P. J. Asiello and A. J. Baeumner, *Lab Chip*, 2011, **11**, 1420–30.

23   J. Brownie, S. Shawcross, J. Theaker, D. Whitcombe, R. Ferrie, C. Newton and S. Little, *Nucleic Acids Res.*, 1997, **25**, 3235–3241.

24   G. T. Walker, *PCR Methods Appl.*, 1993, **3**, 1–6.

25   M. Vincent, Y. Xu and H. Kong, *EMBO Rep.*, 2004, **5**, 795–800.

26   G. T. Walker, M. C. Little, J. G. Nadeau and D. D. Shank, *PNAS*, 1992, **89**, 392–396.

27   W. A. Al-Soud, I. S. Ouis, D. Q. Li, Å. Ljungh and T. Wadström, *FEMS Immunol. Med. Microbiol.*, 2005, **44**, 177–182.

28   L. Kux, *Fed. Regist.*, 2012, **77**, 16124–16125.

29   M. D. Frank-Kamenetskii and S. Prakash, *Phys. Life Rev.*, 2014, **11**, 153–170.

30   E. N. Nikolova, E. Kim, A. a Wise, P. J. O'Brien, I. Andricioaei and H. M. Al-Hashimi, *Nature*, 2011, **470**, 498–502.

31   A. R. Richardson, S. J. Libby and F. C. Fang, *Science*, 2008, **319**, 1672–6.

32   E. A. Lukhtanov, S. G. Lokhov, V. V Gorn, M. A. Podyminogin and W. Mahoney, *Nucleic Acids Res.*, 2007, **35**, e30.

33   M. Ebert, D. Ackermann, S. Pitsch and B. Jaun, *Chimia (Aarau).*, 2001, **55**, 852–855.

34   S. Nierzwicki-Bauer, J. Gebhardt, L. Linkkila and K. Walsh, *Biotechniques*, 1990, **9**, 472–8.

35   S. Kalachikov, B. Adarichev and G. Dymshits, *Russ. J. Bioorganic Chem.*, 1992, **18**, 52–62.

36   G. J. Boggy and P. J. Woolf, *PLoS One*, 2010, **5**, e12355.

37   S. Mehra and W.-S. Hu, *Biotechnol. Bioeng.*, 2005, **91**, 848–60.

38   H. Schmidt and M. Jirstrand, *Bioinformatics*, 2006, **22**, 514–515.

39   N. Panpradist, B. J. Toley, X. Zhang, S. Byrnes, J. R. Buser, J. a. Englund and B. R. Lutz, *PLoS One*, 2014, **9**, e105786.
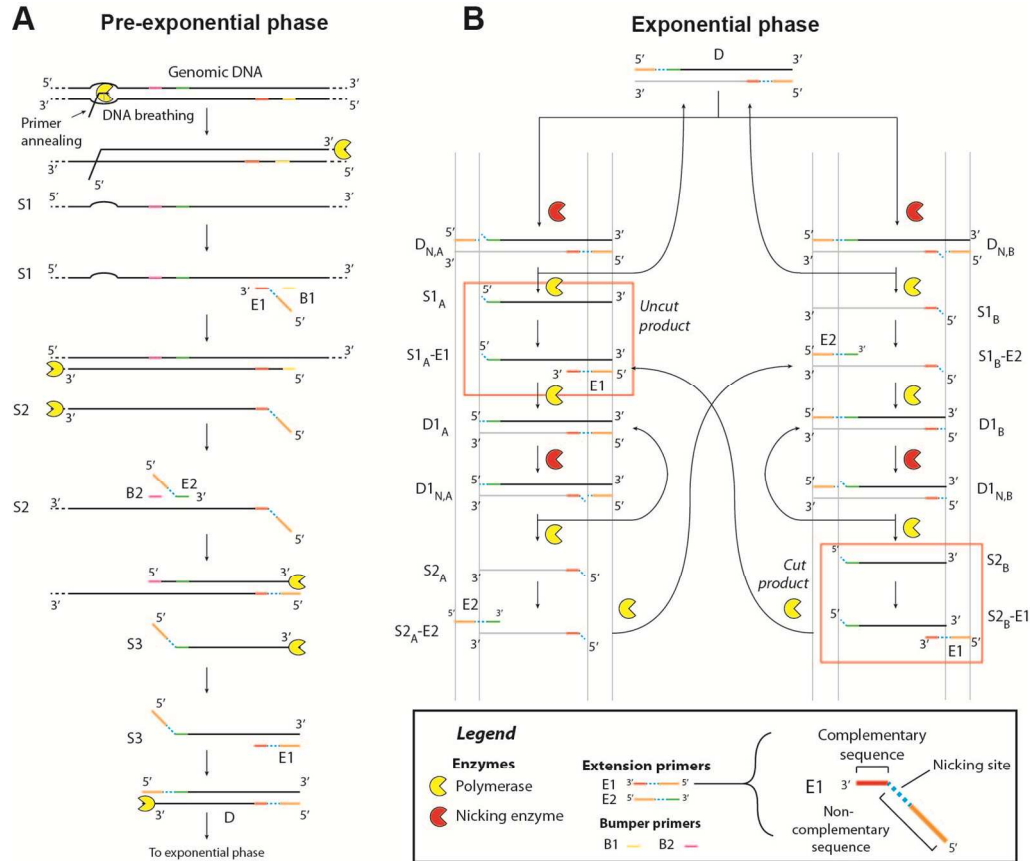
Figures

Figure 1. Proposed molecular mechanism of iSDA. There are two main stages: pre-exponential (**A**) and exponential (**B**). **A**. In the pre-exponential phase, a primer invades double-stranded DNA at a breathing site. The primer is extended by a polymerase, displacing a single strand, S1, which initiates a cascade of subsequent steps involving annealing and extension of two primer pairs (E1, E2, B1, B2), ultimately generating a double-stranded product, D, which has nicking sites (dotted blue sequence; see *Legend*) on both strands. **B**. The exponential phase initiates from species D and involves a set of nicking and extension reactions. The complementary strands of D are denoted by black and grey color. Nicking followed by extension and displacement from the two nicking sites in D generates single stranded products, SA1 and SB1. SA1 and SB1 bind to their corresponding complementary primers and their extension produces double-stranded products DA1 and DB1, respectively, each having a nicking site on one strand. Nicking and extension from these sites generates single strand products SA2 and SB2, respectively. Finally, the corresponding complementary primers anneal to SA2 and SB2 and their extension also regenerates DA1 and DB1. *Legend* shows the different regions of primer E1. Primer E2 has similar regions.
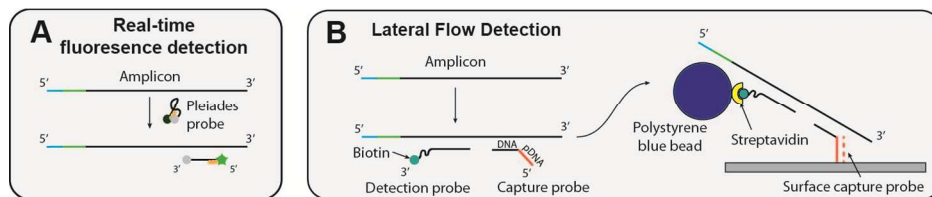
Figure 2. Methods of amplicon detection. **A**. Real-time detection of amplicons using Pleiades fluorescent probes. The Pleiades probes have a fluorophore and minor groove binder at the 5' end and a quencher at the 3' end. They produce low background and high hybridization-triggered fluorescence. **B**. High specificity of lateral flow detection is achieved by using two probes that target two different regions of the amplicon. The detection probe is biotinylated at the 3' end and conjugates with streptavidin-coated beads to produce a visible signal. The capture probe is a hybrid 5'-pDNA-DNA probe. The DNA portion of the probe hybridizes to the amplicon and the pDNA portion hybridizes to a complementary pDNA surface capture probe.
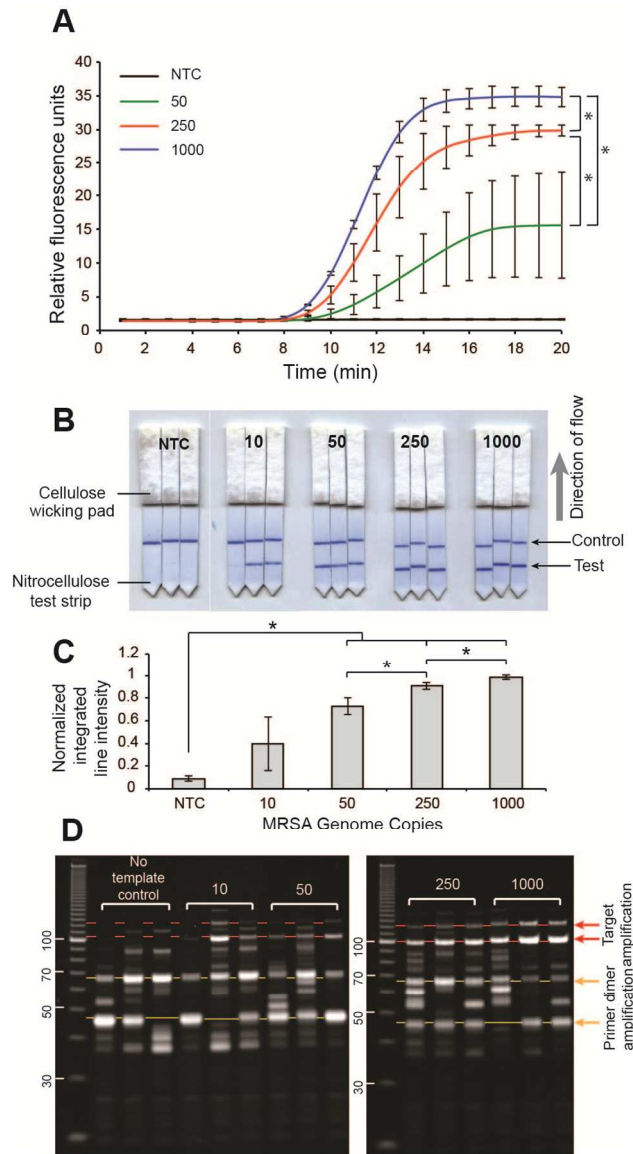
Figure 3. iSDA amplification of MSSA DNA. **A**. Real-time amplification curves of different starting copy numbers of MSSA genomic DNA. Curves are mean of 3 replicates and error bars are standard deviations. **B**. Lateral flow detection of amplification products starting from different copy numbers of MSSA genomic DNA. **C**. Normalized integrated line intensities of lateral flow assay signals. Average signals for 50, 250, and 1000 copies were greater than NTC (*;$P<5x10^{-4}$) and increased significantly with increasing starting copies (*;$P<0.05$). **D**. Denaturing PAGE gel analysis of products shows two target product bands at ~100 and 120 nucleotides (red arrows). There were many side product bands and two bands at ~47 and 67 nucleotides (yellow arrows) were most likely primer dimer amplification bands.
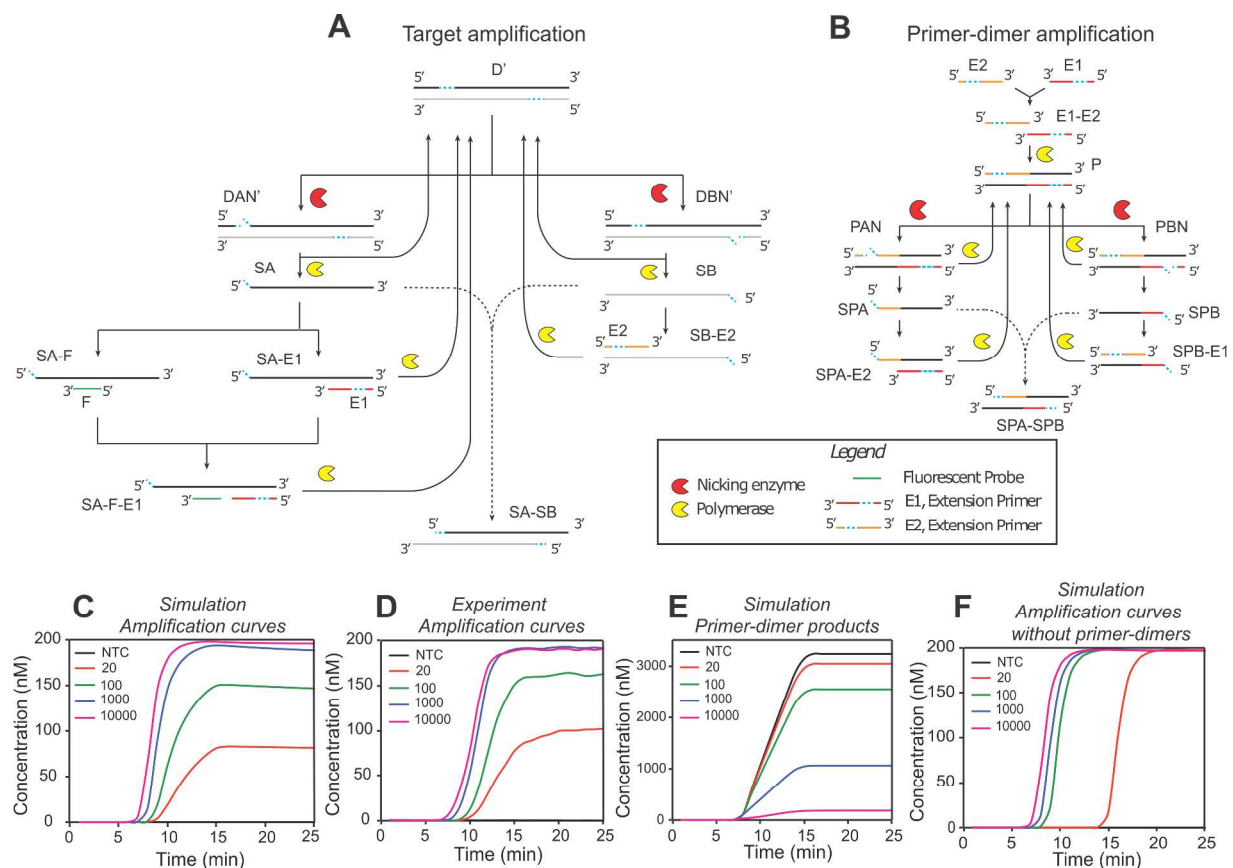
26

Figure 4. A simple mathematical model of iSDA. **A-B**. Simplified schematic of target amplification (**A**) and primer-dimer amplification (**B**). **C-D**. Amplification curves predicted by the model (**C**) and obtained experimentally (average of 3 runs) (**D**) for different starting copies. **E**. Concentration of primer-dimer amplification products (P+PAN+PBN+SPA+SPB+SPA-E2+SPB-E1+SPA-SPB) over time as predicted by the model. **F**. Simulated target amplification curves in absence of primer-dimer amplification as predicted by the model.
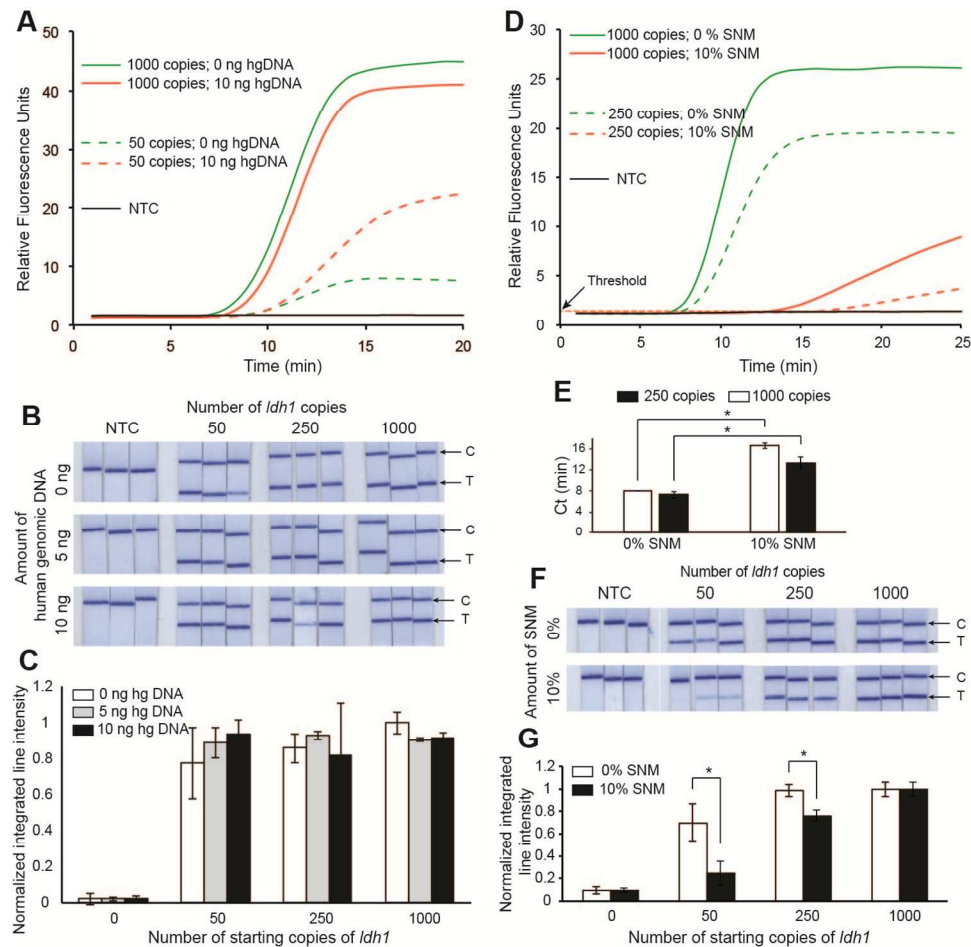
Figure 5. Tolerance of iSDA to contaminants. Figure shows results of iSDA amplification in the presence of human genomic DNA. (**A-C**) and simulated nasal matrix (**D-G). A.** Average (N=3) real-time curves in the presence of 0 and 10 ng hgDNA. **B**. Lateral flow detection of amplification products in the presence of 0, 5, and 10 ng hgDNA. **C**. Integrated signal line intensities from lateral flow in the presence of 0, 5, and 10 ng hgDNA. **D**. Average (N=3) real-time curves in the presence of 0 and 10% SNM. **E**. Ct values of the curves in presence of 10% SNM. 10% SNM significantly increases the Ct value (*,P<0.05). **F**. Lateral flow detection of amplification product in the presence of 0 and 10% SNM. 10% SNM reduced target line intensities at low copies. **G**. Integrated signal line intensities in the presence of 0 and 10 % SNM. Signal line intensities were significantly reduced for 50 and 250 copies (*,P<0.05), but not for 1000 copies, in the presence of 10% SNM.
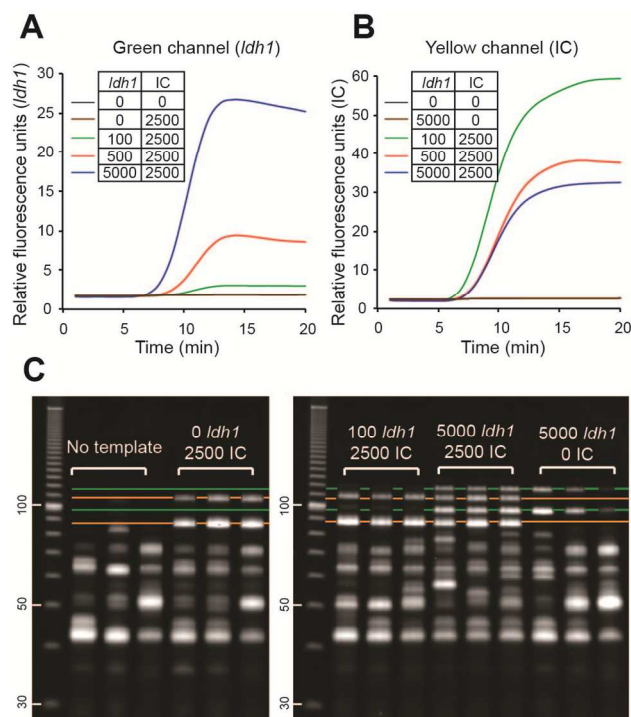
28

Figure 6. Biplexed iSDA amplification. **A**. Amplification curves for different copy numbers of the *ldh1* gene in the presence of 2500 copies of an engineered amplifiable IC sequence. **B**. Amplification curves obtained from 2500 copies of the IC sequence in presence of different copy numbers of the *ldh1* gene. Numbers in table are number of copies. **C**. Denaturing PAGE analysis shows amplification products from *ldh1* (green lines) and IC (yellow lines).